SERI/TP-252-2903
UC Category: 62c
DE86004434

Rapid Heating of Gas/Small-Particle Mixture

K. Y. Wang
W. W. Yuen

February 1986

Prepared for the AIAA/ASME
Heat Transfer and
Thermophysical Conference
Boston, Massachusetts
2-4 June 1986

Prepared under Task No. 5125.210
FTP No. 652

Solar Energy Research Institute
A Division of Midwest Research Institute

1617 Cole Boulevard
Golden, Colorado 80401-3393

Prepared for the
U.S. Department of Energy
Contract No. DE-AC02-83CH10093

Printed in the United States of America
Available from:
National Technical Information Service
U.S. Department of Commerce
5285 Port Royal Road
Springfield, VA 22161

Price: Microfiche A01
Printed Copy A02

Codes are used for pricing all publications. The code is determined by the number of pages in the publication. Information pertaining to the pricing codes can be found in the current issue of the following publications, which are generally available in most libraries: *Energy Research Abstracts, (ERA); Government Reports Announcements* and Index (*GRA* and I); *Scientific and Technical Abstract Reports (STAR);* and publication, NTIS-PR-360 available from NTIS at the above address.

RAPID HEATING OF GAS/SMALL-PARTICLE MIXTURE

K. Y. Wang
Solar Energy Research Institute
Golden, CO 80401

W. W. Yuen
Department of Mechanical & Environmental Engineering
University of California
Santa Barbara, CA 93106

ABSTRACT

The concept of using a mixture of particles and air as a medium to absorb radiative energy has been proposed for various applications. In this paper, carbon particles mixed with gas form a medium that absorbs radiation from sources such as concentrated solar energy. A single-particle, two-temperature model is used to study the transient temperature of the particle/gas mixture as it undergoes a constant pressure expansion process. The results indicate that for particles smaller than 1 μm in diameter, the surrounding air can be heated as quickly as the particles, while for particles larger than 1 mm in diameter, the air temperature stays relatively unchanged and the particles are heated to a very high temperature. The effect of scattering from the particles is also examined, revealing that such a contribution is insignificant for small particles.

NOMENCLATURE

c	specific heat
d	diameter
$e_{b\lambda}$	black body emissive power
f_v	solid direction fraction
G	mass loading factor at initial temperature
h	heat transfer coefficient
Kn	Knudsen number
n	real part of complex refractive index
Nu	Nusselt number
q_R	radiative heat flux
Q_{abs}	absorption efficiency of a spherical particle
Q_{sca}	scattering efficiency of a spherical particle
Q_i	incoming radiative flux
r	radius; distance from an element in the cloud to the center of the particle
s	distance from an element in the cloud to the surface of the particle
t	time
T	temperature

Greek symbols

α	absorptivity; accommodation coefficient
ε	emissivity
κ	imaginary part of complex refractive index
ρ	density
σ	Stefan-Boltzmann constant
σ_{abs}	adsorption coefficient
τ	optical thickness of the cloud
ω	scattering albedo

Subscripts

c	cloud containing particles and gas
g	gas phase
o	initial state

INTRODUCTION

The study of heat transfer for a mixture of particles and gas has been of interest in areas such as airborne aerosol in pollution problems, particle formation in clouds, fluidized beds in combustion chambers, etc. Hunt (1978) proposed the concept of using small particles suspended in a gas to directly absorb solar energy in a cavity for power generation and later (Hunt and Brown 1983) demonstrated in a field test that air temperatures of about 750°C can be achieved when the mixture of air and 0.1-μm-diameter carbon particles are blown through a focal point with 30-kW solar input. More recently, Hruby and coworkers (1983) studied the fundamental characteristics of a solid-particle receiver with intensive radiation input. The free-falling particles with sizes ranging from 300 to 1000 μm were able to achieve a temperature rise of more than 1000°C in a distance about 10 m and a power density of 0.5 MW/m^2. The particle temperature was measured by thermocouples inserted into an insulated bucket that collects particles. The basic concept of a solid-particle receiver is illustrated in Fig. 1.

The purpose of the present study is to quantify the thermal performance of such a particle/air mixture as a function of system inputs such as particle size, density, and flux level. It is also the goal of this study to identify the conditions under which the present model can be applied.

ANALYSIS

The physical configuration of the system under consideration is shown in Fig. 2. A single-direction, uniformly distributed radiation source with intensity Q_i is incident on a cloud of particles. It is assumed that the particles are uniformly suspended in the gas phase and have an average diameter d_p. The characteristic dimension of the cloud is d_c, and $d_c \gg d_p$. The particles are far apart from each other (typical solid fraction $f_v \ll 1$), and therefore the effects of multiple reflection and scattering among the particles are neglected. A simple argument that supports this assumption is summarized in the Appendix. To further simplify the analysis, the convective terms characterizing the relative motions between particles and gas are not presently considered. The above assumptions result in a model that is valid for slow-motion and/or short-time phenomena for a cloud of particles with a low to moderate optical thickness.

A two-temperature model is adapted to analyze the thermal performance of the mixture. The governing equation for the temperature in gas phase T_g is

$$\rho_g c_g \frac{d\,T_g}{dt} = \frac{6h}{d_p} \frac{f_v}{1 - f_v} (T_p - T_g) \ , \qquad (1)$$

and the governing equation for the temperature in the solid phase T_s is

$$\rho_p c_p \frac{d\,T_p}{dt} = \frac{6h}{d_p} (T_g - T_p) - \frac{1}{f_v} \frac{dq_R}{dy} \ . \qquad (2)$$

In Equations (1) and (2), h is the heat transfer coefficient between the solid and gas phase and will be discussed later. The solid fraction f_v is actually a function of temperature, and as the cloud is heated under constant pressure condition, using the ideal gas law, f_v can be expressed as

$$f_v = \frac{G}{\rho_p} \frac{T_g(t = 0)}{T_g(t)} \ , \qquad (3)$$

where G is the initial mass loading of the mixture, defined as the ratio of total solid mass to total mixture volume, and ρ_p is the density of the particle itself. In the calculation, the following properties are used for solid:

$$\rho_p = 2000 \text{ kg/m}^3$$

$$c_p = 712 \text{ J/kgK at 300 K.}$$

The properties of air are used to represent those for the gas phase. The radiative energy change appearing in Equation (2) can be expressed as

$$\frac{dq_R}{dy} = -\frac{3}{2} \frac{1}{d_p} \alpha_p Q_i f_v + \frac{6}{d_p} \varepsilon_p \sigma T_p^4 f_v \ , \qquad (4)$$

based on the radiative energy balance for a single particle.

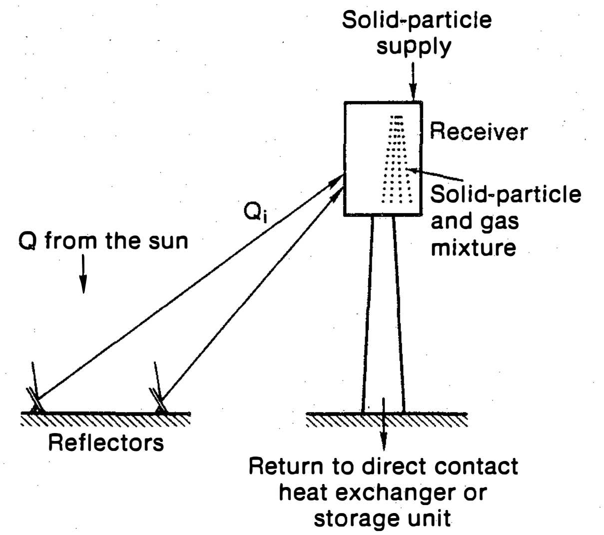

Fig. 1. Solid-particle solar central receiver

In Equation (4), α_p and ε_p are the surface absorptivity and emissivity of the particles and can be determined from the Mie theory for spherical particles (van de Hulst 1957). As previously mentioned, Equation (4) is a very simple form for energy balance, and the effect of radiative attenuation in the cloud has been neglected. Therefore, if the optical thickness of the cloud is large (such as with strong absorption and high particle density), the present model has to be modified to take into consideration the radiation variation along the space coordinate. The initial conditions at t = 0 for Equations (1) and (2) are

$$T_p = T_g = \text{constant} \ . \qquad (5)$$

Equations (1) and (2) can easily be solved numerically using an implicit finite difference method. The gas temperature T_g can be regrouped by taking the solid temperature T_p from Equation (1) and substituting it into Equation (2) so that an expression for T_g can be obtained. It is found that an explicit formulati also results in the same numerical results, but at the expense of a much longer computing time.

In a recent study, Houf and Greif (1985) investigated the radiative transport in a galling sheet of solid particles, similar to the configuration under present investigation. In their analysis, the whole

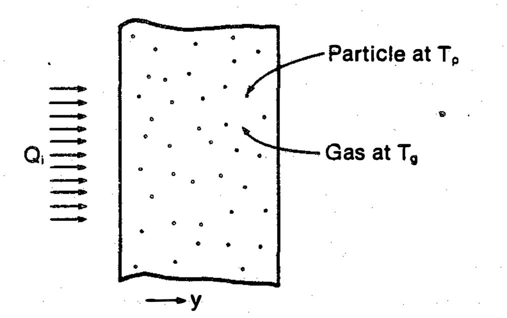

Fig. 2. Physical configuration of the gas and particle mixture receiving radiative input

equation of transfer, rather than the simple expression Equation (4) was used to examine the effect of scattering. However, the transient behavior and thermal interaction between the solid and gas phases were not included. The present analysis examines the problem from another viewpoint, and the condition at which the analysis is applicable will be discussed later.

RESULTS AND DISCUSSION

The optical properties necessary to calculate the radiative properties of the individual particle are the real and imaginary parts of the complex refractive index. Here, the optical properties of carbon are derived from the results measured by Arakawa et al. (1977) and are plotted in Fig. 3 as a function of wavelength. The Mie scattering theory is then used to calculate the absorption efficiency Q_{abs} of the spherical particle (van de Hulst 1957). In the case where the particle size is much larger than the wavelength, the so-called geometric optics regime, the relation

$$Q_{abs} = 1 - \left|\frac{n - i\kappa - 1}{n - i\kappa + 1}\right|^2 \qquad (6)$$

is used as an approximation to save the computing time (Bohren and Hultman 1983), where $i = \sqrt{-1}$.

The total absorption efficiency weighted by the black body emission function for the carbon particle is shown in Fig. 4 as a function of particle diameter. The radiative source is assumed to have a flux distribution the same as a black body at the temperature indicated in the figure. Hence, the curve for T = 5780 K characterizes the absorption of solar radiation by the carbon particle. Similarly, the curves for T = 1000 K and 2000 K characterize the emission from the particle at the designated temperatures. It is the ratio of absorption to emission that quantifies the net energy gain for a particle. The results indicate that particles larger than ~1 μm have a strong ability to absorb radiation, but also lose energy easily by emission at a lower temperature. On the other hand, the energy absorbed by smaller particles is much greater than that emitted from the particle surface. The equivalent emissivity or absorptivity is defined as

$$\varepsilon_p(T) \text{ or } \alpha_p(T) = \frac{1}{\sigma T^4} \int_0^\infty Q_{abs}\, e_{b\lambda}(T)\, d\lambda \ , \qquad (7)$$

where $e_{b\lambda}$ is the black body emissive power.

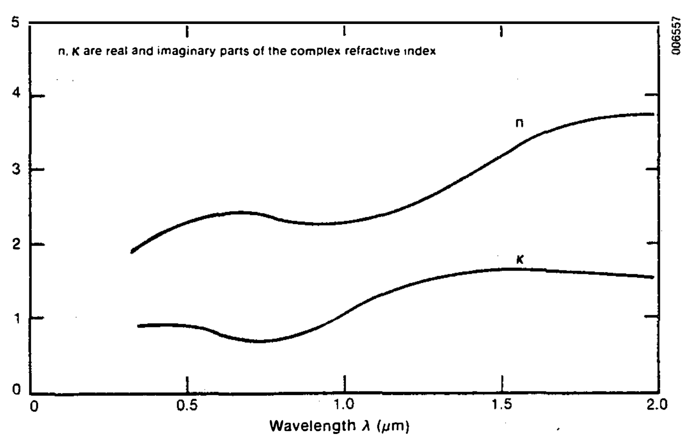

Fig. 3. Optical properties of the carbon particle

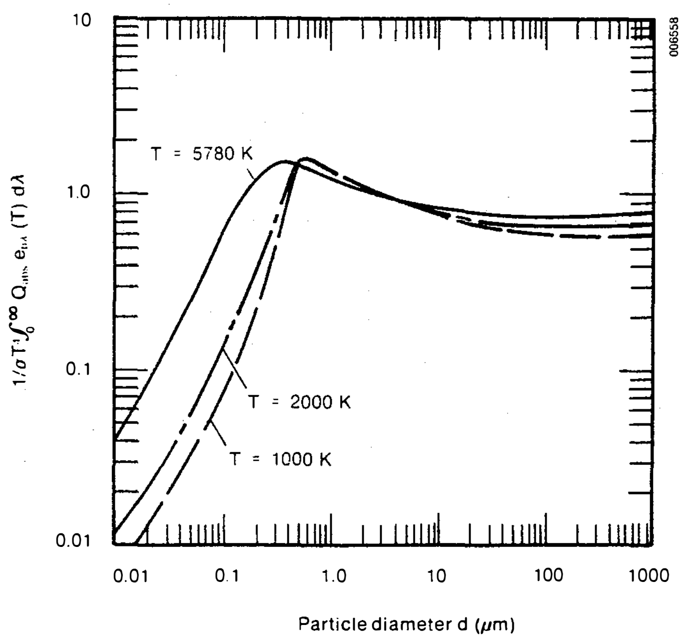

Fig. 4. Absorption efficiency of carbon particles as a function of size

In a recent study, Yuen et al. (1984) investigated the convective heat transfer rate from small particles suspended or immersed in a gas to the surrounding gas. An important dimensionless parameter used in the study is the Knudsen number Kn, defined as the ratio of gas molecule mean free path to d_p, the particle diameter. The mean free path for air is usually extremely small (e.g., <0.1 μm in standard temperature and pressure conditions), but this dimension increases proportional to the absolute temperature. Under the condition Kn << 1, the Nusselt number Nu = 2, which is a familiar result for heat transfer between a particle and motionless fluid. However, as the particle size shrinks to be comparable to the gas mean free path, the heat transfer rate will be reduced since the motions of the gas molecule, which characterize energy transfer by conduction, are hindered. The Nu vs. Kn relation for both monotonic and diatomic gas molecules is presented in Fig. 5. Also shown in Fig. 5 is a value of Nu taken from Clift (1978). The variable α is the accommodation coefficient, which is equal to 1 for perfect accommodation (as the temperature of the gas molecule approaches that of the particle), and is equal to 0 if no energy is exchanged. However, the effect of α on Nu is not very significant under the current study.

The transient temperature of the solid particles and the gas phase are depicted in Fig. 6a and 6b, respectively. It is clear that the highest gas heating rate occurs for the smallest particle/air mixture. This is because the smaller surface-area-to-volume ratio and smaller absorption-to-emission ratio, mentioned above, for the larger particles result in less efficient heat exchange between the solid and gas phases. It is also interesting to note that even in the case of d_p = 1000 μm, where the gas temperature remains essentially unchanged from the initial state, the solid particles are still very efficient in absorbing radiative energy. On the other hand, the combination of a larger-particle/air mixture will be desirable for a solid-particle solar receiver concept as described by Hruby and Steele (1985), where high-

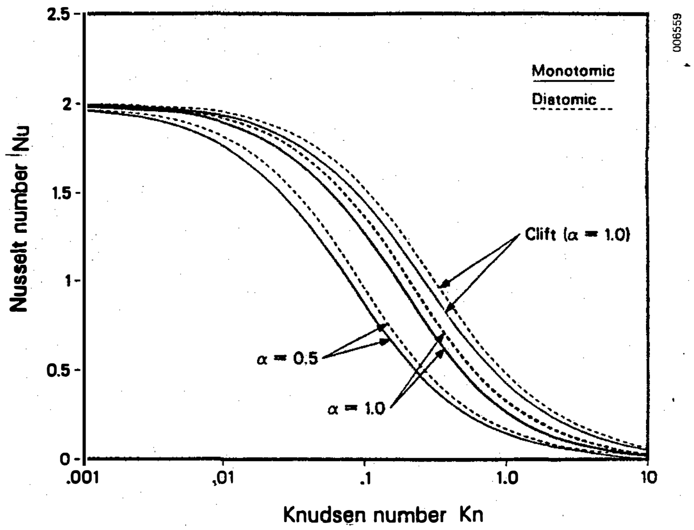

Fig. 5. Nu vs. Kn for spherical particles in a motionless gas (Yuen, et al., 1984). α is accommodation coefficient.

temperature solid particles, not high-temperature air, are the required product. It is also clear from comparing Fig. 6a and 6b that a single-temperature model is acceptable if the solid particles are small (e.g., d_p < 1 μm) in the present case. Adapting this simplification will then allow the model to be expanded easily to take into consideration the radiative attenuation in the space coordinate.

The effect of the particle mass loading factor is shown in Fig. 7. It is evident that the amount of solid particles in the mixture strongly affects the rate of radiation absorbed, thus affecting the heating rate of the gas phase. However, it is also interesting to note that the temperature at steady state, although of little interest as far as the present investigation is concerned, is not changed by the amount of solid particles in the mixture. The present model, which does not consider the scattering effect and radiative attenuation in the mixture, would not be valid as the optical thickness of the cloud becomes appreciable. The absorption coefficient σ_{abs} of the mixture can be expressed as

$$\sigma_{abs} = \frac{3}{2} \frac{Q_{abs}}{d_p} \frac{G}{\rho_p} \frac{T_g\ (t = 0)}{T_g\ (t)} . \qquad (8)$$

This information, together with the dimensions of the cloud d_c, will be sufficient to render the optical thickness of the entire mixture as

$$\tau = \sigma_{abs}\ d_c , \qquad (9)$$

assuming that the particles are uniformly distributed in the cloud. Therefore, as the particle concentration G increases, the present model has to be modified to take into consideration the multiple-particle effects.

The effect of incoming radiative flux Q_i is shown in Fig. 8. The higher flux renders a higher gas temperature, as expected. However, energy loss by radiation at higher temperature is also higher, and this results in less effective energy gain.

The maximum possible temperature difference between the solid and gas phases has been predicted earlier by Yuen et al. (1985). Using the argument that during the heating process the radiative energy absorbed by the particles is always larger than the conductive energy lost to the surrounding gas, and without considering the emission loss by the particle itself, they concluded that

$$T_p - T_g < \frac{Q_i \varepsilon_p}{4\ h} . \qquad (10)$$

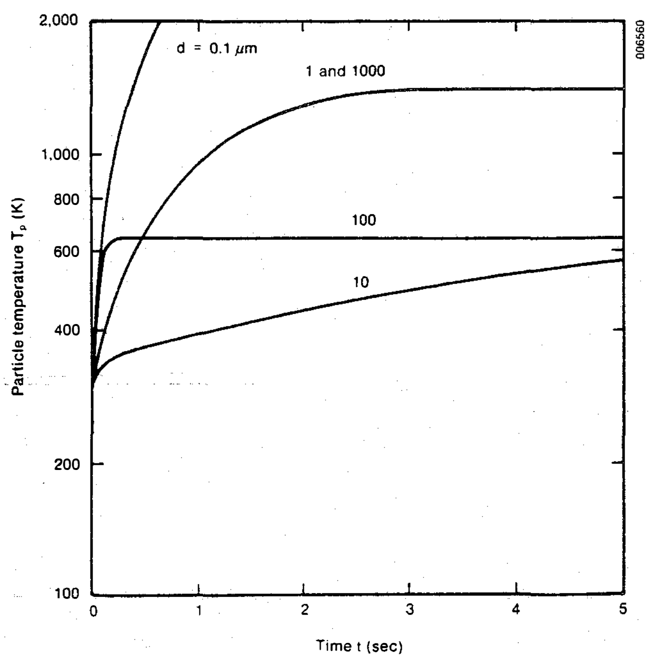

Fig. 6a. Particle temperature **of the mixture after being heated by** $Q_i = 10^6$ **W/m²**. Initial mass loading $G = 10^{-3}$ kg/m³.

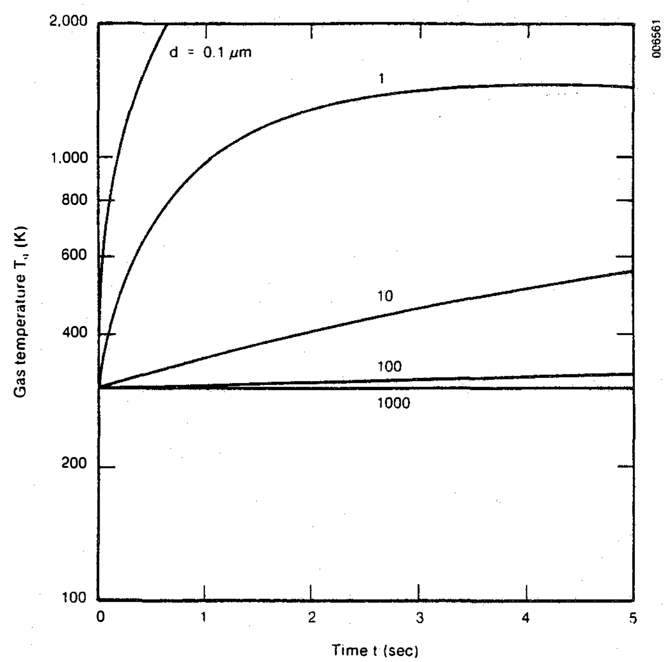

Fig. 6b. Air temperature of the mixture after being heated under the same conditions as in 6a.

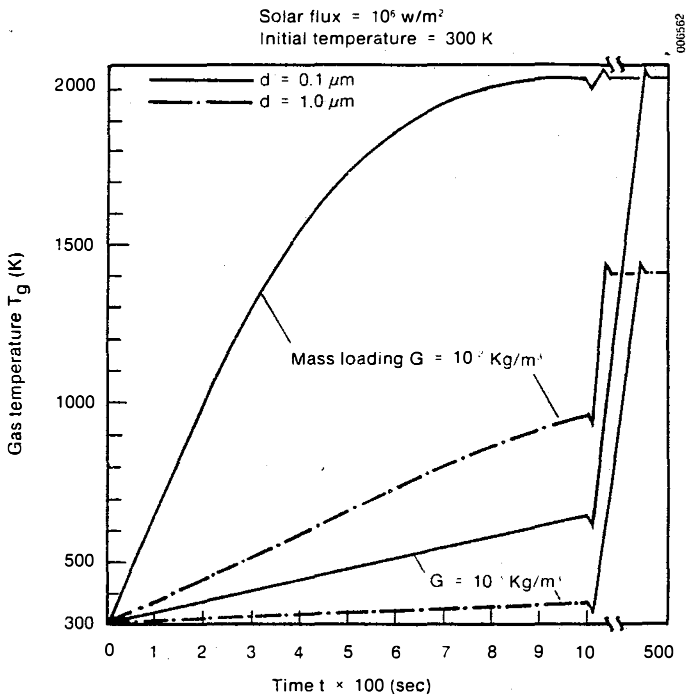

Fig. 7. Effect of mass loading G on air temperature ($Q_i = 10^6 W/m^2$)

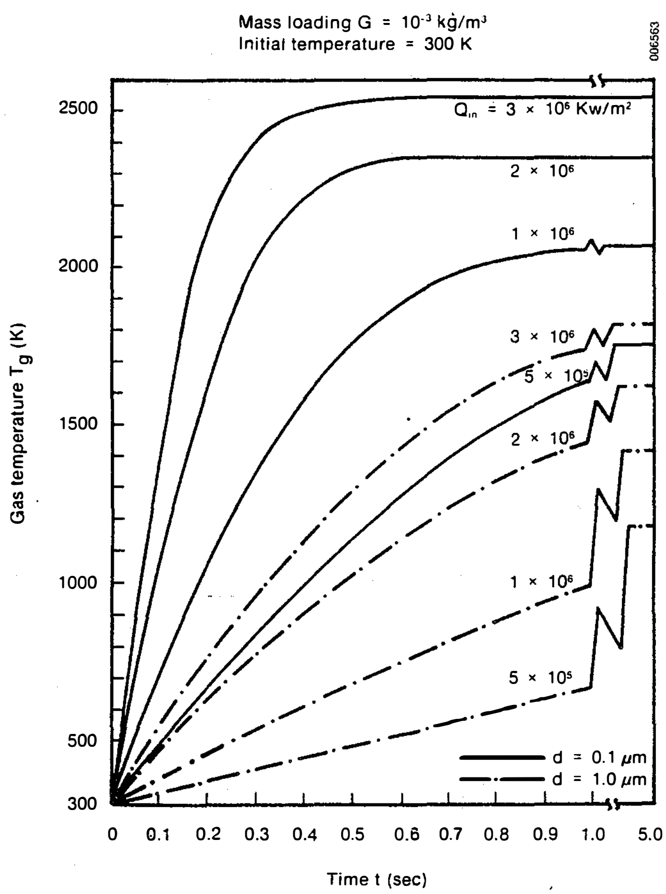

Fig. 8. Effect of incoming radiation flux Q_i on air temperature ($G = 10^{-3}$ kg/m^3)

Their results and the present numerical calculations are listed in Table 1 for comparison. It turns out that the theoretical prediction is satisfactory compared to the numerical results for a small-particle/air mixture. For a large-particle/air mixture the theoretical prediction, although still true, will be less useful.

It was mentioned earlier that the scattering effects are not included in the analysis. The possible contribution from scattering is indicated in Table 2 for different sphere sizes. In the table, Q_{sca} is the scattering efficiency of a single sphere and ω [defined as $Q_{abs}/(Q_{abs} + Q_{sca})$] is the albedo, which indicates the portion where radiation is attenuated by scattering. It is quite clear that the scattering contribution for very small particles (d_p < 0.1 μm) is negligible at lower temperatures. However, it seems that scattering should be included in the analysis if the larger-particle/air mixture is to be used. The results shown in Fig. 6a and 6b for large particles may therefore have been underestimated because of the scattering effects.

The uncertainty in the heat transfer coefficient h is expected to affect the temperatures T_p and T_g. This effect is examined and the results are indicated in Table 3. The particle and air temperatures based on Nu from Fig. 5 are shown there, together with results based on arbitrary Nu. It is quite clear that the effect is very small for small particles for Nu ranging from 0.01 to 2.0, but serious errors may occur if a similar Nu were to be used for larger particles. The heat transfer exchange between the solid and gas phases is very good for small d_p and thus results in the same T_p and T_g values for a wide range of Nu. However, the condition is not true for larger particles, and the temperatures are more sensitive to the Nu chosen.

CONCLUDING REMARKS

This study aims at finding the maximum possible heating rate of the gas phase in a particle/air mixture. A simple two-temperature, transient analysis indicates that very high air temperature (>1000 K) in a very short time (<1 second) appears to be feasible if the particle size, mass loading, and input radiative source are well arranged. It turns out that small par-

Table 1. Comparison of particle-gas temperature difference between the theoretical limits and the numerical computation

	Temperature difference	
d_p (μm)	Theoretical Max. $(T_p - T_g)$ (K)	This work $T_p - T_g$ (K)
0.1	0.8	0
1	2.8	0
10	14.1	9.7
10^2	361.1	274.4
10^3	3610.9	1093.2

Table 2. Radiative properties of the carbon particles (Weighted by the black body emission power)

d_p(μm)	T = 5780 K			T = 2000 K			T = 1000 K		
	Q_{abs}	Q_{sca}	ω	Q_{abs}	Q_{sca}	ω	Q_{abs}	Q_{sca}	ω
0.01	0.042	1.7×10^{-5}	4.2×10^{-4}	0.012	4.8×10^{-7}	4.2×10^{-5}	0.007	1.2×10^{-7}	1.7×10^{-5}
0.1	0.583	0.163	0.219	0.134	0.005	0.037	0.076	0.001	0.016
1	1.253	1.426	0.532	1.343	1.562	0.538	1.358	1.568	0.536
10	0.830	1.350	0.619	0.790	1.488	0.653	0.783	1.519	0.660
100	0.758	1.242	0.621	0.632	1.368	0.684	0.604	1.396	0.698

Table 3. Effect of h on particle and air temperatures

Nu	h (W/m^2 °C)	T_p (K)	T_g (K)
($d_p = 10^{-4}$ m)			
2.0	2.15×10^6	1750.74	1750.70
1.0	1.07×10^6	1750.76	1750.68
0.05*	5.85×10^4	1751.43	1749.98
0.1	1.07×10^5	1751.03	1750.24
0.01	1.07×10^4	1751.66	1745.80
($d_p = 10^{-6}$m)			
2.0	1.02×10^5	682.09	179.21
0.95*	4.88×10^4	685.12	679.05
0.1	5.11×10^3	731.93	675.05
0.01	4.48×10^2	1054.54	570.27
($d_p = 10^{-5}$m)			
2.0	5.58×10^3	363.19	326.15
1.91*	5.33×10^3	364.92	326.16
1.0	2.79×10^3	400.06	326.11
0.1	2.75×10^2	944.88	321.59
0.01	2.62×10^1	1412.21	303.65

*Results from Figure 5.

ticles in the mixture result in a very high heating rate for the air. However, it should be noted that this analysis gives an optimistic heating rate for the mixture because the scattering effect and radiation attenuation in the mixture have been neglected. Since the temperature difference between the small particle (d_p < 1 μm) and the surrounding air is negligible, the present analysis can be modified by adapting a single-temperature model under such circumstances. The simplification will then allow a rigorous transient radiative transfer analysis to be feasible.

REFERENCES

Arakawa, E. T., Williams, M. W., and Inagaki, T., 1977, "Optical Properties of AOC-Evaporated Carbon Films Between 0.6 and 3.8 eV," Journal of Applied Physics, Vol. 48, No. 7, pp. 3176-3177.

Bohren, C. F., and Hultman, D. K., 1983, Absorption and Scattering of Light by Small Particles, Wiley, New York, p. 172.

Clift, R., 1978, Bubbles, Drops and Particles, Academic Press, New York.

Houf, W. G., and Greif, R., 1985, "Radiative Transfer in a Solar Absorbing Particle Laden Flow," presented at the 23rd National Heat Transfer Conference, August 4-7, 1985, Denver, Colo.

Hruby, J. M., and Steel, B. R., 1985, "Examination of Solid Particle Central Receiver: Radiant Heat Experiment," Solar Engineering, pp. 302-308.

Hunt, A. J., 1978, "Small Particle Heat Exchangers" LBL-7841, Lawrence Berkeley Laboratories, Berkeley, Calif.

Hunt, A. J., and Brown, C. T., 1983, "Solar Test Results of an Advanced Direct Absorption High Temperature Gas Receiver," Proceedings of the 8th Biennial Congress of the International Solar Energy Society, Vol. 2, Perth, Australia, pp. 959-963.

van de Hulst, H. C., 1957, Light Scattering by Small Particles, Wiley, New York.

Yuen, W. W., and Hunt, A. J., "Heat Transfer Characteristics of Small Particle/Gas Mixture," to appear in the International Communication of Heat and Mass Transfer.

Yuen, W. W., Miller, F. J., and Hunt, A. J., 1984, "A Two-Zone Model for Conduction Heat Transfer from a Particle to a Surrounding Gas at Arbitrary Knudsen Number," LBL-18449, Lawrence Berkeley Laboratories, Berkeley, Calif.

APPENDIX: ESTIMATE OF RADIATIVE HEAT TRANSFER FROM PARTICLE CLOUDS BACK TO PARTICLE

The amount of radiative energy q_R arriving at a particle surface A_p from the surrounding particle cloud is

$$q_R = \sigma_{abs} \frac{\sigma T_p{}^4}{\pi} \iint \frac{\cos\theta}{s^2} e^{-\tau} \, dA_p dV_s \, . \qquad (11)$$

The details of the relationship between the particle surface d_p and the cloud is depicted in Fig. 9. In this expression, we have assumed that the particle under consideration is at the center of a cell with radius r_g and is surrounded by the particle clouds with diameter R. We have further assumed that radiation is not attenuated in the range $r_p < r < r_g$.

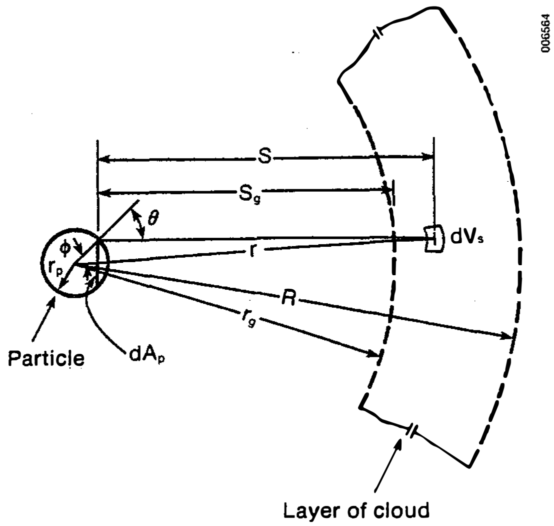

Fig. 9. Relationship between a particle and the surrounding cloud

In Equation (11),

$$dA_p = r_p^2 \sin\phi \, d\phi \, dr$$

$$dV_s = 4\pi r^2 \, dr$$

$$s^2 = r^2 + r_p^2 - 2rr_p \cos\phi$$

$$\tau = \sigma_{abs} (s - s_g) \sim Q_{abs} (r - r_g)$$

$$\sigma_{abs} = \pi r_p^2 \alpha_{abs} N \; ,$$

where N is the number of particles per unit volume and

$$N = \frac{G}{\frac{4}{3}\pi r_p^3 \rho_p} \left(\frac{T_{g,o}}{T_g}\right) .$$

$T_{g,o}$ represents the initial gas temperature and r and s are the distances from an element in the cloud to the center and surface of the particle, respectively.

Substituting these expressions into Equation (11), we obtain

$$q_R = 4\pi r_p^2 \sigma T_p^4 \{1 - \exp(-\tfrac{3}{4} Q_{abs}(r_p/r_g)^2) - \tfrac{3}{2} Q_{abs} (r_p/r_g)^3 \exp(\tfrac{3}{4} Q_{abs}(r_p/r_g)^2) [E_1(\tfrac{3}{4} Q_{abs}(r_p/r_g)^2) - E_1(\tfrac{3}{4} Q_{abs} \frac{R}{r_g} (r_p/r_g)^2)]\} . \quad (12)$$

Notice that the assumptions $R/r_g >> 1$ and $r_p/r_g << 1$ have been used in deriving Equation (12). E_1 represents the exponential integral function:

$$E_1(x) = \int_0^1 1/y \exp(-x/y) \, dy .$$

The ratio r_p/r_g depends on the ratio $(G/\rho_p)^{1/3}$, but is typically less than 5×10^{-3}. The value of q_R in Equation (12) will be significant only when

$$\frac{R}{r_g} (r_p/r_g)^2 Q_{abs} >> 1 .$$

This corresponds to $R >> 10^6 r_g/Q_{abs} = 8 \times 10^6 r_p/Q_{abs}$. For r_p in the range from 0.05 to 0.5 μm, the emission from the cloud to the particle will not be significant unless R > 4 m.